Fluid Phase Equilibria 476 (2018) 16–24

Contents lists available at ScienceDirect

Fluid Phase Equilibria

journal homepage: www.elsevier.com/locate/fluid

A Monte Carlo simulation study of the interfacial tension for water/oil mixtures at elevated temperatures and pressures: Water/*n*-dodecane, water/toluene, and water/(*n*-dodecane + toluene)

Jingyi L. Chen [a], Bai Xue [a], David B. Harwood [a], Qile P. Chen [a, b], Cornelis J. Peters [c], J. Ilja Siepmann [a, b, *]

[a] Department of Chemistry and Chemical Theory Center, University of Minnesota, 207 Pleasant Street SE, Minneapolis, MN 55455-0431, USA
[b] Department of Chemical Engineering and Materials Science, University of Minnesota, 421 Washington Avenue SE, Minneapolis, MN 55455-0132, USA
[c] Department of Chemical Engineering, Petroleum Institute, Khalifa University of Science and Technology, P.O. BOX 2533, Abu Dhabi, United Arab Emirates

ARTICLE INFO

Article history:
Received 27 February 2017
Received in revised form
6 June 2017
Accepted 17 June 2017
Available online 23 June 2017

Keywords:
Monte Carlo simulation
Interfacial tension
n-Dodecane
Toluene
Water

ABSTRACT

Monte Carlo simulations are performed to predict the interfacial tension (IFT) for water/*n*-dodecane, water/toluene, and water/(50 wt% *n*-dodecane + 50 wt% toluene) mixtures at a pressure of 1.83 MPa and temperatures ranging from 383.15 to 443.15 K. Simulations for the binary mixtures are performed in the $N_1N_2p_NAT$ ensemble and those for the ternary mixtures are performed in the $N_1\mu_2\mu_3p_NAT$ ensemble. In order to control the composition of the organic phase for ternary mixture simulations, separate reservoirs for toluene and *n*-dodecane molecules are utilized, and the minimum and maximum numbers of these molecules in the interfacial box are monitored. Identity switch moves are applied to facilitate the sampling of the spatial distributions of the organic molecules. Calculations of the IFT for water/*n*-decane and water/benzene mixtures are used to benchmark the force fields and to develop mixing rules. The combination of the TraPPE–UA force field and the TIP4P/2005 water model with Lorentz-Berthelot combining rules yields fairly accurate predictions at moderate temperatures for water/*n*-decane, but appears to slightly overestimate the IFT at elevated temperatures. For the water/benzene mixtures, the TraPPE–EH//TIP4P/2005 combination significantly overestimates the IFT over the entire temperature range. Subsequent modifications of the energetic Lennard-Jones cross-interaction parameters yield good agreement between experimental and simulated IFT data of water/*n*-decane and water/benzene. Using a preliminary set of modified cross-interaction parameters for the TraPPE–UA/EH//TIP4P/2005 combination, our predictions for the Industrial Fluid Properties Simulation Challenge yield satisfactory agreement with the benchmark data (mean signed errors of −2.2, −5.1, and −0.1 dyn/cm for water/*n*-dodecane, water/toluene, and water/(50 wt% *n*-dodecane + 50 wt% toluene), respectively). A new set of modified cross-interaction parameters developed later based on longer simulation trajectories and a larger set of experimental data is found to reduce the mean signed errors to −0.1, −0.6, and +2.5 dyn/cm, respectively, for these three systems. Although a significant enrichment of toluene molecules at the interface is found for the ternary mixture, this enrichment is not sufficient to reproduce the experimental IFT data.

1. Introduction

This work is carried out to address the 9th Industrial Fluid Properties Simulation Challenge (IFPSC) [1]. The challenge for 2016 was to predict the interfacial tension (IFT) for water/*n*-dodecane, water/toluene, and water/(50 wt% *n*-dodecane + 50 wt% toluene) mixtures at a pressure of 1.83 MPa and four temperatures (383.15, 403.15, 423.15, and 443.15 K). Although water/oil IFTs are crucial for many industrial processes such as enhanced oil recovery [2] and control of detergency [3], experimental measurements of them, especially at elevated temperatures and pressures, remain a challenge [4]. This can be illustrated by the large spread among experimental data obtained by different research groups for the IFT of the water/*n*-decane mixture (see Fig. 1). The difference between

* Corresponding author. Department of Chemistry and Chemical Theory Center, University of Minnesota, 207 Pleasant Street SE, Minneapolis, MN 55455-0431, USA.
E-mail address: siepmann@umn.edu (J.I. Siepmann).

http://dx.doi.org/10.1016/j.fluid.2017.06.015
0378-3812/

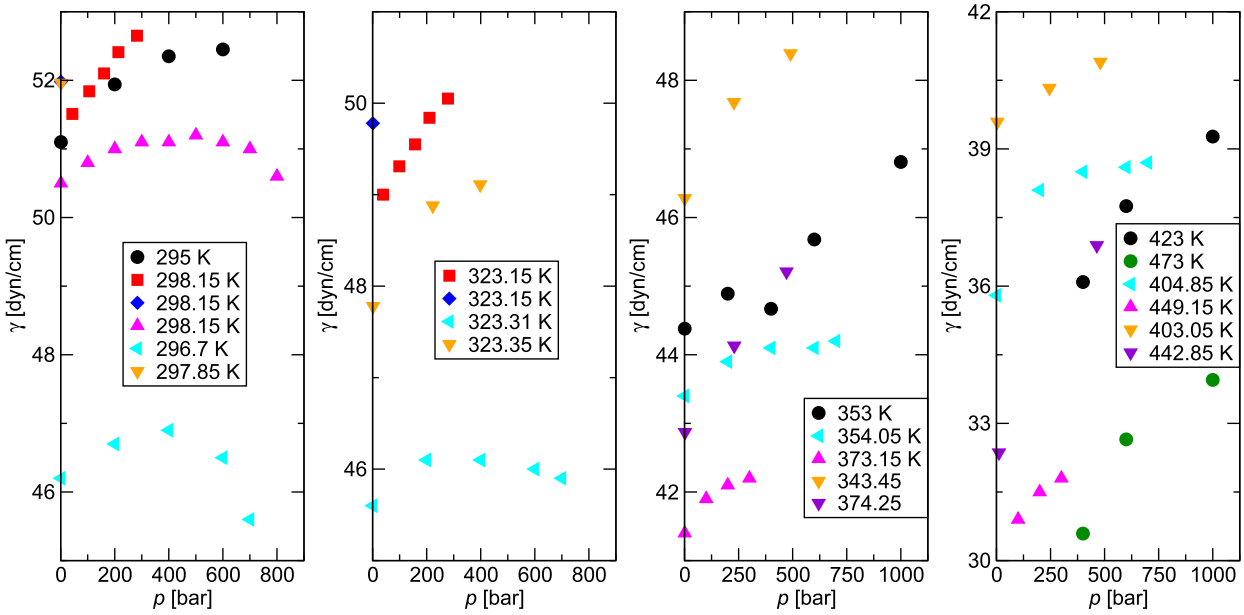

Fig. 1. Experimental IFT data for the water/*n*-decane mixture grouped by temperature ranges. The black and green circles, red squares, blue diamonds, magenta up triangles, cyan left triangles, and orange and purple down triangles denote data reported by Wiegand and Franck [10], Cai et al. [11], Zeppieri et al. [12], Jennings [13], Michaels and Hauser [14], and Georgiadis et al. [15], respectively. Note that the blue diamond and orange triangle are overlapping at 52 dyn/cm in the left panel. (For interpretation of the references to colour in this figure legend, the reader is referred to the web version of this article.)

two data points at essentially the same state point is found to be as large as 6 dyn/cm. The experimental data also show significant differences in the pressure dependence of the IFT.

Molecular simulations may offer a tool to quantitatively predict the IFT of water/oil mixtures at elevated temperatures and pressures. However, at present, the force fields needed for these simulations require parameterization/validation against experimental data for related systems at near-ambient conditions, and the simulations can only partially substitute for experiments at challenging conditions. Furthermore, simulations can also provide molecular-level insight into interfacial enrichment and orientational order. Previous simulation studies for water/oil interfacial systems were mostly concerned with short-chain alkanes and were carried out either at low temperatures or at low pressures [5–9]. Therefore, the 9th IFPSC stimulates an effort to investigate water/oil interfacial systems at both elevated temperatures and pressures. In this work, the accuracy of the combination of the TraPPE force fields for aliphatic and aromatic hydrocarbons with the TIP4P/2005 water model is assessed based on available experimental data for the IFT of water/*n*-decane and water/benzene mixtures. Then modifications of the energetic Lennard-Jones cross-interaction parameters are introduced and the modified force fields are applied to predict the IFT for water/*n*-dodecane, water/toluene, and water/(50 wt% *n*-dodecane + 50 wt% toluene) mixtures at elevated temperatures and pressures.

2. Simulation methods

2.1. Force fields

The Lennard-Jones (LJ) 12–6 and Coulomb potentials are used to describe the intermolecular interactions of water, *n*-alkanes, benzene, and toluene, and also the nonbonded intramolecular interactions for the flexible alkane chains:

$$u_{ij}(r_{ij}) = 4\varepsilon_{ij}\left[\left(\frac{\sigma_{ij}}{r_{ij}}\right)^{12} - \left(\frac{\sigma_{ij}}{r_{ij}}\right)^{6}\right] + \frac{q_i q_j}{4\pi\varepsilon_0 r_{ij}} \quad (1)$$

where r_{ij}, ε_{ij}, σ_{ij}, q_i, q_j, and ε_0 are the distance between interaction sites i and j, the LJ well depth, the LJ diameter, the partial charges on interaction sites i and j, and the permittivity of vacuum, respectively. The modified Lorentz–Berthelot (LB) combining rules [16] are used to determine the LJ parameters for unlike interactions:

$$\varepsilon_{ij} = k_{ij}\sqrt{\varepsilon_{ii}\varepsilon_{jj}} \qquad \sigma_{ij} = \frac{\sigma_{ii} + \sigma_{jj}}{2} \quad (2)$$

where k_{ij} is a parameter used to scale the unlike well depth to mimic departures from the Berthelot rule; $k_{ij} = 1.0$ corresponds to the standard Berthelot combining rule. In all simulations, water is represented by the rigid four-site TIP4P/2005 model [17] because, in addition to overall excellent performance for neat water, this model also yields very accurate predictions for the liquid–vapor surface tension of neat water (with an underprediction of about 3% for 300 K $\leq T \leq$ 450 K [18,19]). *n*-Decane and *n*-dodecane are represented by ten- and twelve-site semi-flexible united-atom models with the interaction parameters taken from the TraPPE–UA force field [20] that is also known to yield accurate predictions for the surface tension (with an over-prediction by about 3% for *n*-heptane [21]). Benzene and toluene are represented by rigid twelve-site models with the interaction parameters for carbon and explicit hydrogen atoms being part of the aromatic ring taken from the TraPPE–EH force field [22] and parameters for the united-atom methyl group of toluene taken from the TraPPE–UA force field [20]. The partial charges of toluene are chosen following the convention used for other substituted aromatic compounds [23]. The Supporting Material (Tables S1 and S2) provides a detailed description of all force field parameters and the charge parameterization procedure. The liquid–vapor surface tension of the TraPPE–EH toluene model is calculated in this work (see Table S3). With regards to the

surface tension (but not to the saturated vapor pressure), the TraPPE–EH toluene model is less accurate than the TIP4P/2005 water and TraPPE–UA alkane models. Averaging over five temperatures ranging from 293.15 to 373.15 K, the TraPPE–EH model over-predicts the surface tension by 14% (see Fig. S1).

2.2. Calculation method used for the interfacial tension

The IFT, γ_{KB}, is calculated based on the Kirkwood and Buff definition [24,25]. The simulations are performed in an elongated (along the z-direction) box with periodic boundary conditions in all three directions that contains two liquid phases and two planar interfaces perpendicular to the z-direction. In this case, γ_{KB} can be determined as follows:

$$\gamma_{KB} = \frac{1}{2}\left\langle P_N - P_T \right\rangle L_z \tag{3}$$

where L_z is the length of the periodic simulation box in the z-direction, P_N and P_T are the normal and tangential components, respectively, of the pressure tensor, and the factor of $1/2$ accounts for the presence of two interfaces in the periodic box.

2.3. Long-range corrections for Lennard-Jones interactions

The Janeček long-range correction [26] is utilized for the LJ part of the energy and pressure calculations, whereas the Ewald summation is used for the Coulomb part (see below). The simulation box is divided into a fixed number, N_s, of thin slabs along the z-direction. In the current work, N_s is set to 400 yielding a slab width of $\Delta z = L_z/400$ that fluctuates in proportion to L_z in the $N_1N_2p_NAT$ and $N_1\mu_2\mu_3p_NAT$ ensembles. The total long-range correction to the potential energy is calculated by summing the contributions from all individual slabs:

$$U_{LRC} = \frac{1}{2}\sum_{n=1}^{N_s} u_{LRC}(z_n) \tag{4}$$

where z_n denotes the position of the center of each slab. The contribution from each slab is calculated from

$$u_{LRC}(z_n) = \sum_{i=1}^{t_{LJ}}\sum_{j=1}^{t_{LJ}} \rho_i(z_n) V_s \sum_{m=1}^{N_s} \rho_j(z_m) w_{ij}(|z_m - z_n|)\Delta z \tag{5}$$

where t_{LJ} is the number of types of Lennard-Jones interaction sites, $\rho_i(z_n)$ and $\rho_j(z_n)$ are the number densities for interaction sites of a specific type in slab n located at z_n, and V_s is the volume of each slab. In the present work, the density profiles are evaluated on the fly during each Monte Carlo trial move (i.e., accounting for minor differences in $\rho(z_n)$ between trial and old configurations).

The function $w_{ij}(|z_m - z_n|)$ is computed via the following equation by assuming a uniform distribution of interaction sites in the slab beyond the spherical potential truncation at R_c:

$$w_{ij}(\zeta) = \begin{cases} 4\pi\varepsilon_{ij}(\sigma_{ij})^2\left[\frac{1}{5}(\sigma_{ij}/R_c)^{10} - \frac{1}{2}(\sigma_{ij}/R_c)^4\right] & \zeta \le R_c \\ 4\pi\varepsilon_{ij}(\sigma_{ij})^2\left[\frac{1}{5}(\sigma_{ij}/\zeta)^{10} - \frac{1}{2}(\sigma_{ij}/\zeta)^4\right] & \zeta > R_c \end{cases} \tag{6}$$

The long-range correction for the IFT is obtained here through calculating the long-range correction for different components of the pressure tensor in an analogous manner. Details can be found in Ref. [26].

2.4. Simulation details

For all simulations in this work, a spherical potential truncation at $R_c = 16$ Å is utilized for the intermolecular LJ interactions. The Ewald summation method [27] is utilized to calculate the Coulomb interactions with a screening parameter of $\kappa = 3.2/R_c$ and an upper bound of the reciprocal space summation at $K_{max,i} = \text{int}(\kappa L_i) + 1$, where i can be x, y, or z and L_i is the length of the corresponding box dimension. An additional hard-sphere potential with $\sigma_{HS} = 1.2$ Å is used to avoid unphysical configurations of two water molecules where a hydrogen site with partial positive charge belonging to one molecule would nearly coincide with the negatively charged M site of another molecule.

All simulations are carried out using the Monte Carlo for Complex Chemical Systems–Minnesota (MCCCS–MN, version 16.1) code developed in house. In order to sample the classical phase space, the following types of moves are performed: center-of-mass translations [28] for all types of molecules, rotations around the center of mass [29] for all types of molecules, conformational changes via the dual cut-off, coupled-decoupled configurational-bias Monte Carlo (DCCD-CBMC) algorithm [30–32] only for alkane molecules, and volume changes with an external reservoir [33]. For simulations of the ternary mixture, particle transfers are performed using DCCD-CBMC with multiple trial sites for the insertion of the first bead [31,32,34,35]. During the equilibration period, the maximum displacements are adjusted to yield an acceptance ratio of about 40% for translational, rotational and volume moves. The probabilities of each type of move are distributed to approximately reflect the number of degrees of freedom of each type to be sampled. Details about the distribution of move probabilities are provided in Tables S4 and S5.

Simulations for the parametrization of k_{ij}. Water/n-decane and water/benzene IFT simulations with the normal and modified LB combining rules are run to assess the accuracy of the force fields. The simulations are carried out in the isobaric-isothermal ensemble with fixed interfacial area ($N_WN_Op_NAT$, where the subscripts W and O denote water and organic compounds). These simulations are initialized using the following procedure. First, simulations in the canonical (NVT) ensemble are performed to obtain stable liquid configurations for unary systems consisting of 1500 water, 150 n-decane, or 290 benzene molecules using the same box size of $32 \times 32 \times 50$ Å^3 for all three systems. Then the water box is appended to the n-decane (or benzene) box along the z-direction. After the water and n-decane (or benzene) boxes are combined, the system is briefly equilibrated in the canonical (N_WN_OVT) ensemble to remove energetically unfavorable configurations. Thereafter, the simulations are switched to the $N_WN_Op_NAT$ ensemble and only the z-dimension of the simulation box is allowed to fluctuate. The binary systems are further equilibrated in the $N_WN_Op_NAT$ ensemble for at least 50,000 Monte Carlo cycles (MCCs), where one MCC consists of N randomly chosen MC moves, where $N = N_W + N_O$ is the total number of molecules in the system. For the k_{ij} parameters used for the challenge entry, statistics are gathered from 8 independent simulations, each consisting of at least 100,000 MCCs for production. After submission of the IFPSC entry, the lengths of the production periods are extended to ensure that the uncertainty of each data point is reduced to be less than 2.1 dyn/cm, and additional low-temperature, low-pressure state points were investigated to find improved k_{ij} parameters.

Simulations for binary mixtures. Simulations for water/n-dodecane and water/toluene mixtures are performed in the $N_WN_Op_NAT$ ensemble at $T = 383.15$, 403.15, 423.15, 443.15 K and $p_N = 1.83$ MPa. These systems contain 1500 water molecules and either 120 n-dodecane or 260 toluene molecules. The cross-sectional area of the simulation box is 1024 Å^2 with $L_x = L_y = 32$

Å. The simulations are set up using the procedure outlined above for the water/*n*-decane and water/benzene mixtures. Statistics for the IFT prediction are gathered from 16 independent simulations, each consisting of at least 140,000 MCCs for the production periods. The predictions using this simulation protocol are denoted in the following sections as O1. After the submission of the IFPSC entry, simulations with the same k_{ij} parameters are all elongated to 200,000 MCCs for the production period. The predictions using this simulation protocol are denoted in the following sections as O2. Furthermore, 16 independent simulations with the improved k_{ij} parameters are also carried out using 200,000 MCCs for the production periods. The predictions using this simulation protocol are denoted in the following as I2.

Simulations for ternary mixtures. Considering the finite size of the simulated system, a different set-up is needed for the ternary mixtures to ensure that the bulk region of the organic phase maintains the desired composition even for situations where one component exhibits preferential adsorption at the interface. Simulations for the water/(50 wt% *n*-dodecane + 50 wt% toluene) mixture are carried out in the $N_W\mu_D\mu_T p_N AT$ ensemble, where the subscripts D and T denote *n*-dodecane and toluene, respectively. In order to control the organic-phase composition, the simulations with the MCCCS–MN software utilize a 3-box $N_W N_D N_T (p_N A) p_D p_T T$ osmotic Gibbs ensemble set-up [35–37] (see Fig. S2 for an illustration of the simulation set-up). The elongated liquid box that contains the two interfaces is initialized following the same procedure as for the binary simulations, but replacing the neat organic phase with a 50 wt% *n*-dodecane + 50 wt% toluene mixture. Only the *z*-dimension of the liquid box is allowed to fluctuate with p_N = 1.83 MPa. In order to facilitate sampling of the spatial distribution of the *n*-dodecane and toluene molecules in the organic-phase region, identity switch moves with the DCCD-CBMC algorithm [38–41] are performed utilizing two types of intermediate impurities: 3-methyl-pentane and *n*-octane; only one molecule of each impurity type is introduced into the liquid-phase box and these molecules are not allowed to transfer into another box.

The other two boxes are separate ideal-gas reservoirs for *n*-dodecane and toluene molecules, respectively, and these molecules are allowed to transfer between the liquid-phase box and their corresponding reservoirs to equilibriate their chemical potentials. The reasons for using reservoirs with explicit molecules but all intermolecular interactions switched-off are three-fold. First, the dual cut-off CBMC formalism reduces computational demands for particle transfer and conformational moves, but does not allow for the calculation of chemical potentials via the Rosenbluth weights [31]. Second, the calculation of Gibbs free energies of transfer is more precise and less prone to finite-size effects than the calculation of excess chemical potentials [42]. Third, the volume of the liquid-phase box is allowed to fluctuate in response to the normal pressure, whereas the standard grand canonical ensemble requires a fixed volume.

The external pressures, p_D and p_T, of the separate *n*-dodecane and toluene ideal-gas reservoirs are set to be equal to those corresponding to the number densities of ideal-gas reservoirs that are in contact with a 50/50 wt% toluene and *n*-dodecane bulk (i.e., no interfaces) liquid mixture at p = 1.83 MPa and a specific temperature. Isotropic volume moves are used to maintain the pressure of these ideal-gas reservoirs.

The pressures p_D and p_T are determined by the following procedure. First, several sets of 3-box $N_D N_T p_{liq} V_D V_T T$ Gibbs ensemble simulations are carried out using a cubic liquid-phase box and two separate ideal gas reservoirs both with fixed volume for *n*-dodecane and toluene molecules, respectively (see Fig. S3 for an illustration of the simulation set-up). Simulations are performed at four temperatures using multiple different *n*-dodecane/toluene overall numbers of molecules in the system: 159/241, 150/250, 146/254, and 140/260 (corresponding to weight ratios 54.9/45.1, 52.6/47.4, 51.5/48.5, and 49.9/50.1 wt%, respectively). The simulations are set up with all molecules initially placed in the liquid-phase box, and isotropic volume moves are performed on this box in contact with an external pressure reservoir at p = 1.83 MPa. *n*-Dodecane and toluene molecules are allowed to transfer between the liquid-phase box and their corresponding ideal-gas reservoirs. In order to improve the statistics, the sizes of the vapor boxes are adjusted throughout the equilibration period, so that they contain on average approximately 20 molecules. Statistics are gathered from 8 independent simulations, each consisting of 100,000 MCCs for the production period. Fig. 2 (numerical data are provided in Table S6) shows the calculated average number densities of toluene and *n*-dodecane molecules in their corresponding ideal-gas boxes as function of the average mole fraction in the liquid phase at all four pressure-temperature conditions. The ideal-gas number densities of toluene and *n*-dodecane molecules that correspond to a 50/50 wt

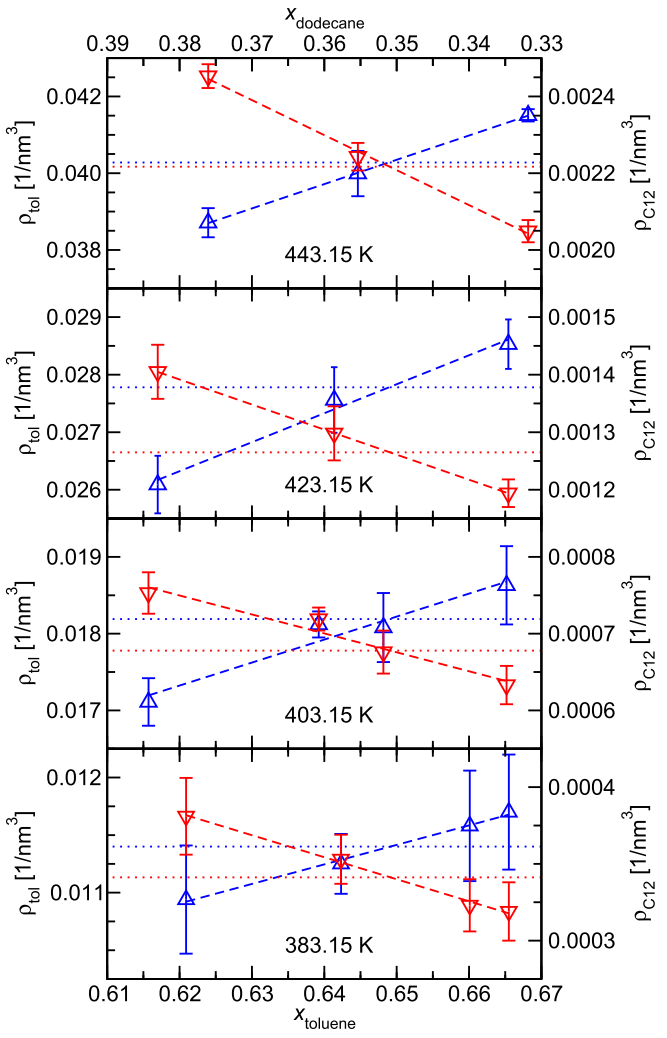

Fig. 2. Ideal-gas number densities of toluene (blue up triangles) and *n*-dodecane (red down triangles) reflecting the corresponding chemical potentials as function of toluene mole fraction in the liquid phase at T = 383.15, 403.15, 423.15 and 443.15 K, and p = 1.83 MPa. Dashed lines show linear fits of the data and the dotted-lines indicate the ideal gas number densities for a 50/50 wt% ($x_{toluene}$ = 0.649) mixture. (For interpretation of the references to colour in this figure legend, the reader is referred to the web version of this article.)

% ($x_{toluene} = 0.649$) in the liquid-phase box are determined through linear interpolation, and then converted into pressures using the ideal gas law (numerical data can be found in Table S7).

As for the binary mixtures, predictions for the ternary mixture are based on 16 independent simulations, and these are performed using the protocols O1, O2, and I2.

With the set-up used here for the ternary mixture, one concern is that the global free energy minimum would be a state with most of the organic molecules in their ideal-gas reservoirs and a single aqueous phase in the elongated box (i.e., the free energy cost for the two interfaces would be removed). To this end, we monitor the number of *n*-dodecane and toluene molecules in the liquid-phase box. Of course, the fluctuations in the numbers of the two types of organic molecules are coupled through the volume of the organic region (plus an offset due to interfacial enrichment). For the current simulations the number of *n*-dodecane molecules is found to range from 31 to 77 and those for toluene from 91 to 179 with the extrema observed at the highest temperature. Thus, the current trajectories would not have been affected by hard lower boundaries of 30 *n*-dodecane and 90 toluene molecules. In addition, we performed another set of simulations at $T = 423.15$ K with the improved set of k_{ij} parameters during which volume moves are not used for the liquid box, i,e., an $N_W N_D N_T V_{liq} p_D p_T T$ Gibbs ensemble. In this case, the external pressure is maintained through the transfers of *n*-dodecane and toluene molecules with chemical potentials that combine to a bulk liquid-phase pressure of 1.83 MPa. Since the free energy cost for the water/vapor surface is larger than that for the water/organic interface and the volume of the aqueous region is constrained by the number of water molecules, the remainder of the elongated box will always be occupied by a liquid region of the organic components. The IFT values obtained with fluctuating and fixed volume for the liquid-phase box are found to be statistically indistinguishable, thereby confirming that the approach using a fluctuating volume is valid as long as the fluctuations are constrained either through a hard boundary or through a sufficient nucleation free energy barrier.

3. Results and discussion

Parametrization of k_{ij}. IFT data assessing the accuracy of the IFT predictions with the TraPPE–UA/EH//TIP4P/2005 combination of force fields are shown in Fig. 3 (numerical data are provided in Tables S8–S11). Using the standard LB combining rule ($k_{ij} = 1.00$), it is found that the IFT for the water/*n*-decane mixture is slightly underestimated at $T = 323$ K and $p = 1$ bar compared to the experimental data reported by Zeppieri et al. [12], but overestimated by about 10% at elevated temperatures and pressures compared to the experimental data reported by Wiegand and Franck [10]. In contrast, the IFT for the water/benzene mixture is overestimated by factors of 1.6 and 2.1 at $p = 20.0$ MPa and $T = 373$

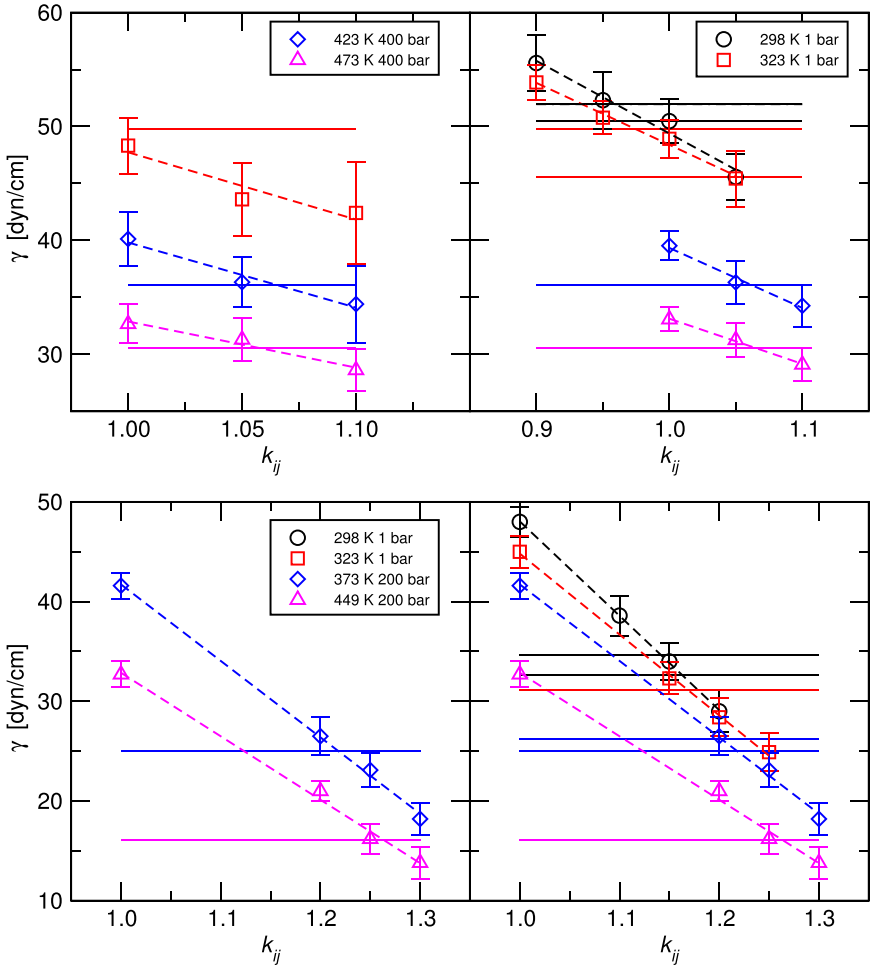

Fig. 3. Determination of k_{ij} parameters. The left column shows the IFT data for the water/*n*-decane (top) and the water/benzene (bottom) mixtures versus k_{ij} at different state points that are used for the k_{ij} parameterization of the IFPSC entry. The right column shows IFT data obtained from longer simulations and also at additional state points that are used for the subsequent improved k_{ij} parameterization. Horizontal lines indicate specific values and upper/lower bounds of experimental data [10–15].

and 449 K, respectively, compared to the experimental data reported by Jennings [13]. The large overestimation of the water/benzene IFT can likely be attributed to two main factors. Assuming that the surface tension of benzene is over-predicted to a similar extent as that for toluene, then this shortcoming of the TraPPE–EH model would contribute significantly to the overestimation of the water/benzene IFT. The other factor is the use of non-polarizable force fields that apparently do not capture the significant polarization of the π-electrons (and weak charge transfer due to hydrogen bond formation) in the highly polarizable aromatic ring. In contrast, *n*-decane is less polarizable and also does not act as an electron donor for the formation of hydrogen bonds, and the TraPPE–UA model only slightly over-predicts the surface tension of alkanes.

One approach to implicitly account for induced polarization effects is to modify the Berthelot combining rule for unlike interactions, and a few studies have already tried to increase the scaling parameter k_{ij} to improve water/alkane mutual solubilities [5,43–46]. Therefore, additional simulations for the water/*n*-decane mixture are run exploring $k_{ij} = 1.05$ and 1.10 for the cross interaction between the O atom in water (only the oxygen site carries a LJ interaction in the TIP4P/2005 water model) and the $-CH_3$ and $-CH_2-$ groups in *n*-decane. Similarly, simulations for the water/benzene mixture are run using $k_{ij} = 1.20$, 1.25, and 1.30 for the interactions between the oxygen site in water and the aromatic interaction sites at carbon and hydrogen nuclei in the TraPPE–EH benzene model. The IFT data for both water/*n*-decane and water/benzene mixtures indicate a weak temperature dependence with larger deviations from the standard Berthelot rule at higher temperatures (and pressures). Nevertheless, the state-point independent k_{ij} values for our IFPSC entry are determined by averaging the values corresponding to the intersections of the selected experimental data (three and two state points for water/*n*-decane and water/benzene, respectively) and linear fits to the k_{ij} -dependent calculated IFT data. Furthermore, the same k_{ij} value is used for the $-CH_3$ group of toluene as for the *n*-alkanes. The selected k_{ij} values are summarized in Table 1.

After the submission of the IFPSC entry, some changes are made to the determination of k_{ij} parameters to improve the accuracy of the predictions. First, to reflect the presumably higher accuracy of experimental data at near-ambient conditions, additional state points are incorporated for both water/*n*-decane and water/benzene mixtures, so that two low-temperature/low-pressure state points and two high-temperature/high-pressure state points are used for each mixture. Second, longer production periods and additional k_{ij} values were used to improve the precision of the k_{ij} parameterization. Third, multiple experimental values at the selected state points are used for the determination of the intersection points. In order to account for the differences in the number of experimental data sources among the chosen state points, the improved k_{ij} values are obtained as follows: An unweighted average of the intersection points for multiple experimental values at a given state point is calculated. Then, a weighted average is calculated from these state-point specific k_{ij} values with the weights proportional to the square root of the number of experimental data available at that state point. Fourth, since the $-CH_3$ group in toluene replaces a hydrogen site in benzene, the corresponding k_{ij} is taken to be the average between O–CH_x (aliphatic) and O–C (aromatic). Another choice would have been to fit different k_{ij} values for the carbon and hydrogen sites of benzene with, maybe, the latter using the same k_{ij} value as for the alkanes.

One concern with the procedure described above is whether one should indeed give equal weight to different experimental data sets. For the case of the water/alkane mixture, Georgiadis et al. [15] recently provided a critical review of the experimental data. When considering only the low-temperature data measured and recommended by Georgiadis et al. for the parameterization of k_{ij} for the O–CH_x(aliphatic) interactions, then we obtain $k_{ij} = 1.00$ instead of 1.01. The difference between these two values is small but, more importantly, also indicates that an increase of k_{ij} with increasing temperature may be advantageous.

Prediction of IFT for binary and ternary mixtures. The IFT predictions from the current simulation study are presented in Fig. 4 and numerical data are provided in Table 2. It should be emphasized first that the statistical uncertainties in the calculated IFT values are quite large; the 95% confidence intervals range from 1.1 to 2.3 dyn/cm and correspond to relative uncertainties in the range from 3 to 7%. Since the IFT values decrease on average only by 10% as the temperature is increased by 20 K, there is considerable scatter in the data over this narrow temperature interval. On the other hand, it should be noted that the spread of experimental data between independent measurements from different groups also indicates combined uncertainties of about 2 dyn/cm (see Fig. 1).

To smooth out the noise in the predicted IFT data (e.g., the values at $T = 383.15$ and 403.15 K for the water/toluene mixture show an increase with increasing temperature that is unphysical for a regular miscibility gap ending in an upper critical solution point), our IFPSC entry is based on a linear fit to the data at the four temperatures. The IFT values of our IFPSC entry underpredict the experimental benchmark data by a mean signed error (MSE) of −2.2 dyn/cm (mean unsigned percentage error (MUPE) of 6%) for the water/*n*-dodecane mixture and with MSE of −5.1 dyn/cm (MUPE of 21%) for the water/toluene mixture, whereas the predictions for the ternary mixture are in fortuitously excellent agreement with an MSE of only −0.1 dyn/cm (MUPE of 3%). MSE and MUPE are defined by the following equations,

$$\mathrm{MSE} = \frac{1}{N_T}\sum_{n=1}^{N_T}\left(\gamma_{\mathrm{sim},n} - \gamma_{\mathrm{ben},n}\right) \tag{7}$$

$$\mathrm{MUPE} = \frac{100\%}{N_T}\sum_{n=1}^{N_T}\frac{\left|\gamma_{\mathrm{sim},n} - \gamma_{\mathrm{ben},n}\right|}{\gamma_{\mathrm{ben},n}} \tag{8}$$

where *n* labels the different state points with $N_T = 4$ temperatures considered in the present case; $\gamma_{\mathrm{sim},n}$ and $\gamma_{\mathrm{ben},n}$ are calculated and benchmark IFT values, respectively. The longer simulations with the same k_{ij} parameters reduce the MUPEs only very slightly to 5, 20, and 3%, respectively, thus any failures are due to the model and not due to insufficient statistics. The underprediction for both binary mixtures indicates that the k_{ij} parameters used for our IFPSC

Table 1
k_{ij} values used for the IFT predictions.

	O/CH_x		O/(C or H)
	alkane	toluene	aromatic ring
IFPSC entry	1.03	1.03	1.25
Improved values	1.01	1.10	1.19

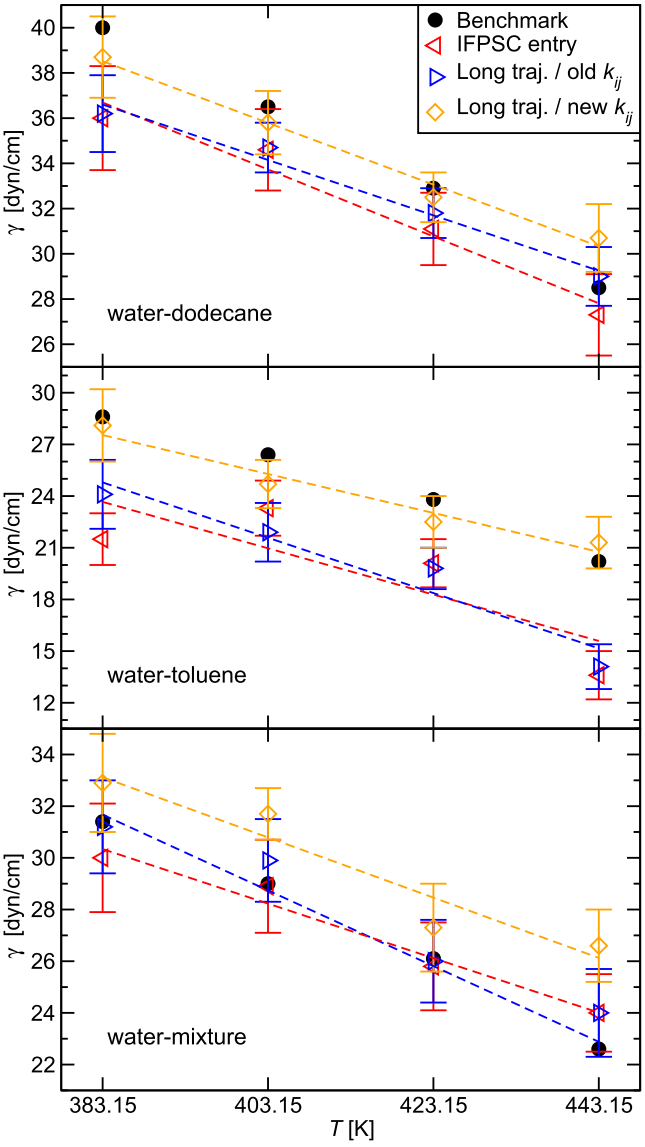

Fig. 4. Predicted IFT data for water/*n*-dodecane, water/toluene, and water/(50 wt% toluene + 50 wt% *n*-dodecane) as function of temperature at $p = 1.83$ MPa. Open symbols denote averages obtained from Monte Carlo simulations at a specific state point, dashed lines represent the linear fits using all four temperatures, and filled black circles denote the benchmark data. The red left triangles, blue right triangles, and orange diamonds correspond to data obtained with the O1, O2, and I2 simulation protocols. (For interpretation of the references to colour in this figure legend, the reader is referred to the web version of this article.)

entry are too large and over-correct the IFT. Our IFPSC predictions yield values for the ternary mixture that exceed the average of the two binary mixtures by a factor of 1.05. In contrast, for the benchmark data, the IFT of the ternary mixture falls below the average of the binary mixtures by a factor of 1.09. The positive excess IFT for the ternary mixture found for our IFPSC entry indicates that adjusting k_{ij} parameters for the LJ interactions leads to a global effect (explicitly up to the cut-off and implicitly through the tail corrections), whereas a more local effect may be needed to yield a negative excess IFT (see below).

As is evident from Fig. 4, the improved k_{ij} parameters based on additional state points and longer simulations yield vastly better IFT predictions for the two binary mixtures with MSEs of only −0.1 and −0.6 dyn/cm (MUPEs of 4 and 5%) for the water/*n*-dodecane and water/toluene mixtures, respectively. However, the MSE and MUPE for the ternary mixture are now +2.5 dyn/cm and 9%, respectively. With the improved k_{ij} parameters, the predictions for the ternary mixture exceed the average of the two binary mixtures only by a factor of 1.01, which is still a positive excess IFT.

Table 2
Benchmark and simulation data of the IFT (in units of dyn/cm) for the water/*n*-dodecane (W/D), water/toluene (W/T), and water/(50 wt% toluene + 50 wt% *n*-dodecane) (W/DT) mixtures at four temperatures and $p = 1.83$ MPa. The uncertainties denote the 95% confidence intervals. The data in bold font are our IFPSC entry. In the Protocol column, the letters A and L stand for the average obtained from 16 independent simulations at a specific state point or the value determined from a linear fit to the averages at all state points.

Mixture	Protocol	T [K]			
		383.15	403.15	423.15	443.15
W/D	Benchmark	40.0	36.5	32.9	28.5
	O1A	36.0 ± 2.3	34.6 ± 1.8	31.1 ± 1.6	27.3 ± 1.8
	O1L	**36.7** ± **1.6**	**33.7** ± 1.1	**30.8** ± 1.2	**27.8** ± 1.7
	O2A	36.2 ±1.7	34.7 ± 1.1	31.8 ± 1.1	29.0 ± 1.3
	I2A	38.7 ± 1.8	35.8 ± 1.4	32.5 ± 1.1	30.7 ± 1.5
W/T	Benchmark	28.6	26.4	23.8	20.2
	O1A	21.5 ± 1.5	23.3 ± 1.6	20.1 ± 1.4	13.6 ± 1.4
	O1L	**23.7** ± 1.9	**21.0** ± 1.1	**18.3** ± 1.0	**15.6** ± 1.6
	O2A	24.1 ± 2.0	21.9 ± 1.7	19.8 ± 1.2	14.1 ± 1.3
	I2A	28.1 ± 2.1	24.7 ± 1.4	22.5 ± 1.5	21.3 ± 1.5
W/DT	Benchmark	31.4	29.0	26.1	22.6
	O1A	30.0 ± 2.1	28.9 ± 1.8	25.8 ± 1.7	24.0 ± 1.5
	O1L	**30.3** ± 1.3	**28.2** ± 1.0	**26.1** ± 1.1	**24.0** ± 1.6
	O2A	31.2 ± 1.8	29.9 ± 1.6	26.0 ± 1.6	24.0 ± 1.7
	I2A	32.9 ± 1.9	31.7 ± 1.0	27.3 ± 1.7	26.6 ± 1.4

Since induced polarization and charge transfer would mostly influence interactions between molecules in close proximity of each other, we also investigate a modification with a distance-dependent $k_{ij}(r)$ parameter that only acts on short-ranged interactions between the water oxygen atom and the carbon atoms of the aromatic ring (protocol I3, see Supporting Material for a detailed description). Use of protocol I3 yields MSEs of +0.3 and +2.3 dyn/cm (MUPEs of 3 and 8%) for binary water/toluene and ternary mixtures, and the IFT of the ternary system is now slightly smaller (by 1%) than the average of the two binary mixtures. Although the distance-dependent $k_{ij}(r)$ parameter yields a negative excess IFT, the small change is within the statistical uncertainties of the simulation data. The small difference between protocols I2 and I3 indicates that the over-prediction of the surface tension of neat toluene may be the major contributor to the failure to observe a negative excess IFT.

For the predictions with the improved k_{ij} parameters, the IFT values at $T = 383.15$ K exceed those at 443.15 K by factors of 1.26, 1.32, and 1.24 (note that the last digit is not statistically significant) for water/*n*-dodecane, water/toluene, and the ternary mixture, respectively. These factors are somewhat smaller than those for the benchmark data (1.40, 1.42, and 1.39, respectively). However, both experimental data and predictions agree that there is no significant difference in the relative decrease of the IFT for the three mixtures over the temperature range studied. The underprediction of the temperature dependence for the IFT also agrees with the observations made throughout the k_{ij} parameterization (see Fig. 3). Using temperature-independent k_{ij} parameters leads to a slight over-correction (underestimation of the IFT) at lower temperatures, while the opposite holds at higher temperatures. Allowing the k_{ij} parameters to increase with temperature would also increase the temperature dependence for the IFT of the three mixtures.

Interfacial enrichment for the ternary mixture. Since the IFT

of the binary water/*n*-dodecane mixture significantly exceeds that of the water/toluene mixture, one may expect an enrichment of toluene molecules at the water/organic interface for the ternary mixture. To provide molecular-level insight, the toluene weight fraction is determined as function of relative *z*-position in the elongated liquid-phase box; here the center of mass of the water region is calculated for each individual configuration and used to align the profiles. As illustrated by the composition profiles shown in Fig. 5, the simulations indeed yield a significant toluene enrichment at the water/organic interface. This interfacial enrichment decreases with increasing temperature, e.g., the maximum values of the local toluene weight fraction are 0.77 and 0.70 at $T =$ 383.15 and 443.15 K, respectively. The enrichment only extends over about 10 Å before the bulk composition of the organic phase imposed by the reservoirs is reached, and the width of the region with the enhanced toluene concentration increases with decreasing temperature.

Numerical values for the composition of the entire organic region, w_T, and for the bulk-like organic region, w_T^b, in the liquid-phase box are provided in Table 3. At the three higher temperatures, w_T^b is close to 50 wt%, the desired composition for the ternary mixture. At $T = 383.15$ K, however, $w_T^b \approx 48$ wt% for both sets of k_{ij} parameters. This points to a problem with the specific reservoir pressures used at this state point, but it should be noted that the relative uncertainties in the ideal-gas number densities are significantly larger at $T = 383.15$ K (see Fig. 2) and 50 wt% likely falls within the combined uncertainty.

More importantly, the fact that $w_T \geq 57$ wt% for all four state points and both sets of k_{ij} parameters demonstrates the need to carry out simulations for the ternary mixture either in an open ensemble to control the composition or using an extremely large system size so that any interfacial enrichment does not lead to a significant depletion of the interfacilly more active component in the bulk-like organic region (see also Table S13). The average enrichment factors (w_T/w_T^b) for the current system size are found to be essentially the same for the k_{ij} parameters of our IFPSC entry and the improved set (1.158 and 1.155, respectively).

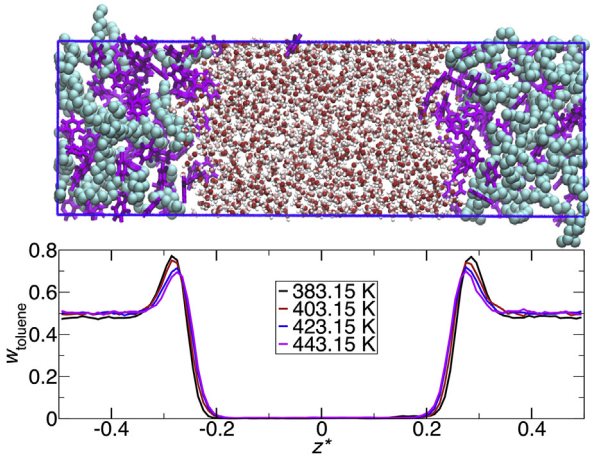

Fig. 5. Interfacial structure for the ternary mixture using the improved k_{ij} parameters. (Top) Snapshot of a representative configuration at $T = 443.15$ K, where the oxygen and hydrogen atoms of water molecules are shown as red and white spheres, respectively, the toluene and *n*-dodecane molecules are represented as magenta wireframes and cyan spheres for the united atoms, respectively. Bottom: Toluene weight fraction profile along the *z*-dimension. The center of mass of the water region is shifted to 0, and z^* is the scaled *z*-coordinate with $z^* = z/L_z$. (For interpretation of the references to colour in this figure legend, the reader is referred to the web version of this article.)

Table 3
Toluene weight fraction in the entire organic region, w_T, and only within the bulk-like part, $|z^*| \geq 0.4$, of the organic region, w_T^b, of the elongated liquid-phase box. The uncertainties denote the 95% confidence intervals.

Region	Protocol	T [K]			
		383.15	403.15	423.15	443.15
w_T [%]	O2	56.5±0.3	58.3±0.4	58.6±0.2	57.4±0.3
w_T [%]	I2	57.0±0.3	57.8±0.2	57.4±0.2	57.0±0.2
w_T^b [%]	O2	48.2±0.6	50.3±0.4	50.7±0.3	50.1±0.3
w_T^b [%]	I2	48.1±0.4	49.9±0.3	50.3±0.3	50.2±0.2

4. Conclusion

This work demonstrates a simulation protocol to predict the interfacial tension of water/oil mixtures that can account for the interfacial enrichment of some components of the oil mixture. The TIP4P/2005// TraPPE–UA combination of force fields can yield fairly accurate results for the water/alkane IFT, whereas the TIP4P/2005// TraPPE–EH combination significantly overestimates the IFT for water/arene mixtures. Although modifications of the energetic Lennard-Jones cross-interaction parameters can lead to a more accurate prediction of the IFTs for binary mixtures, care should be taken when fitting k_{ij} parameters to account for uncertainties in the experimental data. Furthermore, the current study indicates a weak state-point dependence of the binary k_{ij} parameters. Nevertheless, when the state points for the k_{ij} parameterization are chosen appropriately and long simulation trajectories are used, then mean signed errors for the IFT of the water/*n*-dodecane and water/toluene mixtures are found to be less than 1 dyn/cm.

With regards to the prediction of the IFT for the water/(50 wt% *n*-dodecane + 50 wt% toluene) mixture, it needs to be emphasized that the simulations with both sets of k_{ij} parameters yield a value that slightly exceeds the average of the two binary mixtures. That is, we observe a positive excess IFT for the ternary mixture despite the significant enrichment of toluene at the interface, whereas the experimental data demonstrate a negative excess IFT. This observation points to a failure of using non-local k_{ij} parameters to compensate for very local induced polarization and charge transfer effects.

Acknowledgements

We thank the reviewers for valuable feedback. Financial support from the Abu Dhabi Petroleum Institute Research Center (ADPIRC) and computational resources from the Minnesota Supercomputing Institute (MSI) at the University of Minnesota are gratefully acknowledged.

Appendix A. Supplementary data

Supplementary data related to this article can be found at http://dx.doi.org/10.1016/j.fluid.2017.06.015.

References

[1] Industrial Fluid Property Simulation Collective, http://fluidproperties.org.
[2] M. Bavière, Basic Concepts in Enhanced Oil Recovery Processes, Springer, Netherland, 1991.
[3] S.S. Chadwick, Ullmann's Encyclopedia of Industrial Chemistry, Wiley, New York, 2006.
[4] W. Sachs, V. Meyn, Pressure and temperature dependence of the surface tension in the system natural gas/water – principles of investigation and the first precise experimental data for pure methane/water at 25 °C up to 46.8 MPa, Colloid Surf. A 94 (1995) 291–301.
[5] A.R. van Buuren, S.J. Marrink, H.J.C. Berendsen, A molecular dynamics study of the decane/water interface, J. Phys. Chem. 97 (1993) 9206–9212.

[6] D. Michael, I. Benjamin, Solute orientational dynamics and surface roughness of water/hydrocarbon interfaces, J. Phys. Chem. 99 (1995) 1530–1536.
[7] J.L. Rivera, C. McCabe, P.T. Cummings, Molecular simulations of liquid–liquid interfacial properties: water–*n*-alkane and water-methanol–*n*-alkane systems, Phys. Rev. E 67 (2003) 011603.
[8] J.P. Nicolas, N.R. De Souza, Molecular dynamics study of the *n*-hexane–water interface: towards a better understanding of the liquid–liquid interfacial broadening, J. Chem. Phys. 120 (2004) 2464–2469.
[9] F. Biscay, A. Ghoufi, V. Lachet, P. Malfreyt, Monte Carlo calculation of the methane-water interfacial tension at high pressures, J. Chem. Phys. 131 (2009) 124707.
[10] G. Wiegand, E.U. Franck, Interfacial tension between water and non-polar fluids up to 473 K and 2800 bar, Ber. Bunsen. Phys. Chem. 98 (1994) 809–817.
[11] B.-Y. Cai, J.-T. Yang, T.-M. Guo, Interfacial tension of hydrocarbon + water/brine systems under high pressure, J. Chem. Eng. Data 41 (1996) 493–496.
[12] S. Zeppieri, J. Rodríguez, A.L. López de Ramos, Interfacial tension of alkane + water systems, J. Chem. Eng. Data 46 (2001) 1086–1088.
[13] H.Y. Jennings Jr., The effect of temperature and pressure on the interfacial tension of benzene-water and normal decane-water, J. Colloid Interface Sci. 24 (1967) 323–329.
[14] A.S. Michaels, E.A. Hauser, Interfacial tension at elevated pressure and temperature. II. interfacial properties of hydrocarbon-water systems, J. Phys. Chem. 55 (1951) 408–421.
[15] A. Georgiadis, G. Maitland, J.P.M. Trusler, A. Bismarck, Interfacial tension measurements of the (H_2 O + n-decane + CO_2) ternary system at elevated pressures and temperatures, J. Chem. Eng. Data 56 (2011) 4900–4908.
[16] G.C. Maitland, M. Rigby, E.B. Smith, Intermolecular Forces: Their Origin and Determination, Pergamon Press, Oxford, 1987.
[17] J.L.F. Abascal, C. Vega, A general purpose model for the condensed phase of water: TIP4P/2005, J. Chem. Phys. 123 (2005) 234505.
[18] C. Vega, E. de Miguel, Surface tension of the most popular models of water by using the test-area simulation method, J. Chem. Phys. 126 (2007) 154707.
[19] J. Alejandre, G.A. Chapela, The surface tension of TIP4P/2005 water model using Ewald sums for the dispersion interactions, J. Chem. Phys. 132 (2010) 014701.
[20] M.G. Martin, J.I. Siepmann, Transferable potentials for phase equilibria. 1. united-atom description of *n*-alkanes, J. Phys. Chem. B 102 (1998) 2569–2577.
[21] B. Chen, J. I. Siepmann, K. J. Oh, M. L. Klein, Simulating vapor-liquid nucleation of n-alkanes, J. Chem. Phys. 116(2202) 4317–4329.
[22] N. Rai, J.I. Siepmann, Transferable potentials for phase equilibria. 9. Explicit-hydrogen description of benzene and 5-membered and 6-membered heterocyclic aromatic compounds, J. Phys. Chem. B 111 (2007) 10790–10799.
[23] N. Rai, J.I. Siepmann, Transferable potentials for phase equilibria. 10. Explicit-hydrogen description of substituted benzenes and polycyclic aromatic compounds, J. Phys. Chem. B 117 (2013) 273–288.
[24] J.G. Kirkwood, F.P. Buff, The statistical mechanical theory of surface tension, J. Chem. Phys. 17 (1949) 338–343.
[25] A. Ghoufi, P. Malfreyt, D.J. Tildesley, Computer modelling of the surface tension of the gas-liquid and liquid-liquid interface, Chem. Soc. Rev. 45 (2016) 1387–1409.
[26] J. Janeček, Long range corrections in inhomogeneous simulations, J. Phys. Chem. B 110 (2006) 6264–6269.
[27] M.P. Allen, D.J. Tildesley, Computer Simulation of Liquids, Oxford university press, Oxford, 1989.
[28] N. Metropolis, A.W. Rosenbluth, M.N. Rosenbluth, A.H. Teller, E. Teller, Equation of state calculation by fast computing machines, J. Chem. Phys. 21 (1953) 1087–1092.
[29] J.A. Barker, R.O. Watts, Structure of water: a Monte Carlo calculation, Chem. Phys. Lett. 3 (1969) 144–145.
[30] J.I. Siepmann, D. Frenkel, Configurational bias Monte Carlo: a new sampling scheme for flexible chains, Mol. Phys. 75 (1992) 59–70.
[31] T.J.H. Vlugt, M.G. Martin, B. Smit, J.I. Siepmann, R. Krishna, Improving the efficiency of the configurational-bias Monte Carlo algorithm, Mol. Phys. 94 (1998) 727–733.
[32] M.G. Martin, J.I. Siepmann, Novel configurational-bias Monte Carlo method for branched molecules. Transferable potentials for phase equilibria. 2. united-atom description of branched alkanes, J. Phys. Chem. B 103 (1999) 4508–4517.
[33] A.Z. Panagiotopoulos, N. Quirke, M. Stapleton, D.J. Tildesley, Phase equilibria by simulation in the Gibbs ensemble: alternative derivation, generalization and application to mixture and membrane equilibria, Mol. Phys. 63 (1988) 527–545.
[34] G.C.A.M. Mooij, D. Frenkel, B. Smit, Direct simulation of phase equilibria of chain molecules, J. Phys. Condens. Matter 4 (1992) L255–L259.
[35] K. Esselink, L.D.J.C. Loyens, Parallel Monte Carlo simulations, Phys. Rev. E 51 (1995) 1560–1568.
[36] A.Z. Panagiotopoulos, Direct determination of phase coexistence properties of fluids by Monte Carlo simulation in a new ensemble, Mol. Phys. 61 (1987) 813–826.
[37] D.N. Theodorou, Molecular simulations of sorption and diffusion in amorphous polymers, in: P. Neogi (Ed.), Diffusion in Polymers, Marcel Dekker, New York, 1996, pp. 67–142.
[38] J.J. De Pablo, J.M. Prausnitz, Phase equilibria for fluid mixture from Monte-Carlo simulation, Fluid Phase Equilib. 53 (1989) 177–189.
[39] J.I. Siepmann, I.R. McDonald, Monte Carlo simulations of mixed monolayers, Mol. Phys. 75 (1992) 255–259.
[40] M.G. Martin, J.I. Siepmann, Predicting multicomponent phase equilibria and free energies of transfer for alkanes by molecular simulation, J. Am. Chem. Soc. 119 (1997) 8921–8924.
[41] P. Bai, J.I. Siepmann, Selective adsorption from dilute solutions: Gibbs ensemble Monte Carlo simulations, Fluid Phase Equilib. 351 (2013) 1–6.
[42] M.G. Martin, J.I. Siepmann, Calculating Gibbs free energies of transfer from Gibbs ensemble Monte Carlo simulations, Theor. Chem. Acc. 99 (1998) 347–350.
[43] L.R. Pratt, D. Chandler, Theory of the hydrophobic effect, J. Chem. Phys. 67 (1977) 3683–3704.
[44] E. Johansson, K. Bolton, D.N. Theodorou, P. Ahlström, Monte Carlo simulations of equilibrium solubilities and structure of water in *n*-alkanes and polyethylene, J. Chem. Phys. 126 (2007) 224902.
[45] H. Docherty, A. Galindo, C. Vega, E. Sanz, A potential model for methane in water describing correctly the solubility of the gas and the properties of the methane hydrate, J. Chem. Phys. 125 (2006) 074510.
[46] D. Ballal, P. Venkataraman, W.A. Fouad, K.R. Cox, W.G. Chapmann, Isolating the non-polar contribution to the intermolecular potential for water–alkane interactions, J. Chem. Phys. 141 (2014) 064905.